

Recent Advances in Shell Evolution with Shell-Model Calculations

Yutaka UTSUNO^{1,2}, Takaharu OTSUKA^{3,2,4}, Yusuke TSUNODA³, Noritaka SHIMIZU², Michio HONMA⁵, Tomoaki TOGASHI², and Takahiro MIZUSAKI⁶

¹*Advanced Science Research Center, Japan Atomic Energy Agency, Tokai, Ibaraki 319-1195, Japan*

²*Center for Nuclear Study, University of Tokyo, Hongo Tokyo 113-0033, Japan*

³*Department of Physics, University of Tokyo, Hongo, Tokyo 113-0033, Japan*

⁴*National Superconducting Cyclotron Laboratory, Michigan State University, East Lansing, MI 48824, USA*

⁵*Center for Mathematical Sciences, University of Aizu, Ikki-machi, Aizu-Wakamatsu, Fukushima 965-8580, Japan*

⁶*Institute for Natural Sciences, Senshu University, Tokyo 101-8425, Japan*

E-mail: utsuno.yutaka@jaea.go.jp

(Received)

Shell evolution in exotic nuclei is investigated with large-scale shell-model calculations. After presenting that the central and tensor forces produce distinctive ways of shell evolution, we show several recent results: (i) evolution of single-particle-like levels in antimony and copper isotopes, (ii) shape coexistence in nickel isotopes understood in terms of configuration-dependent shell structure, and (iii) prediction of the evolution of the recently established $N = 34$ magic number towards smaller proton numbers. In any case, large-scale shell-model calculations play indispensable roles in describing the interplay between single-particle character and correlation.

KEYWORDS: exotic nuclei, shell evolution, large-scale shell-model calculation, magic number

1. Introduction—shell evolution due to the nuclear force

The evolution of shell structure in nuclei, often called shell evolution, attracts much interest in recent investigations in the physics of exotic nuclei [1–3]. Shell evolution can be accessed through the systematics of an isotope (isotone) chain, where the proton (neutron) Fermi surface is kept unchanged. Such systematic data along long isotope chains are being taken due to recent advances in experiment using radioactive-ion (RI) beams, and they disclose various phenomena that indicate quite sharp shell evolution compared to that of the conventional one-body potential. The most prominent case is the breakdown of the traditional magic numbers including the disappearance of the $N = 20$ magic number known as “island of inversion” [4] and the emergence of an $N = 16$ magic number [5].

While shell evolution is considered as a universal property of nuclei, its complete behavior over the nuclear chart is still ambiguous. This is partly because extracting the evolution of single-particle levels from experiment is not straightforward even in the vicinity of the magic numbers. For instance, having the proton number 51, antimony isotopes are sometimes considered to have nearly pure proton single-particle states in the low-lying energy region [6]. On the other hand, it has been pointed out [2] that those single-particle-like states are strongly mixed with the states involving core excitation (core-coupled states) because typical 2_1^+ and 3_1^- excitation energies in tin isotopes are ~ 1 and ~ 2 MeV, respectively, being close to single-particle-energy spacings. This possible mixing with the core-coupled state makes it difficult to quantify the single-particle levels without resorting to large-scale nuclear-structure calculations which suitably treat many-body correlations including collective 2^+

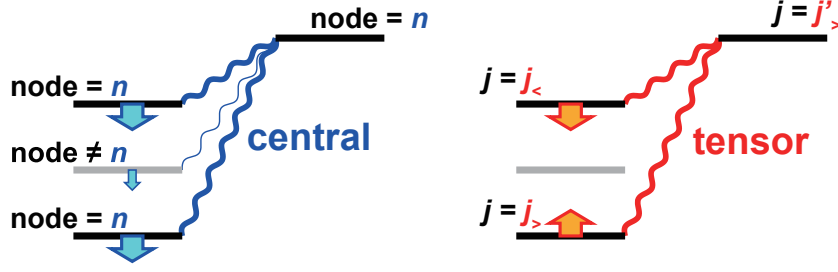


Fig. 1. Schematic illustration of shell evolution caused by the central and tensor proton-neutron forces.

and 3^- states.

The phenomena of shell evolution call for a new mechanism of the formation of shell structure beyond the conventional one-body potential picture. The role of the nuclear force has recently received much attention. If two nucleons in the orbits i and j receive mean attraction whose strength is larger than other pairs, then the i orbit becomes bound more deeply than the others when the orbit j is occupied. Here, mean attraction or repulsion stands for angular-momentum averaged two-body matrix elements called the monopole interaction [7]. In Fig. 1, two major sources that cause the shell evolution in the proton-neutron channel—the central force and the tensor force—are presented together with their effects on the shell structure. Those forces induce very different shell evolutions. The central force, whose effect has been known for a long time (see [8] for instance), gives rise to a stronger attraction between the nucleons in the orbits of the same node. Its dependence on spin direction is rather weak. The tensor force, on the other hand, produces the monopole matrix elements that are opposite in sign between the spin-orbit partners $j_> = l + 1/2$ and $j_< = l - 1/2$ due to the identity $(2j_> + 1)v_{j_>,j}^T + (2j_< + 1)v_{j_<,j}^T = 0$ derived by Otsuka *et al.* in 2005 [9], where $v_{i,j}^T$ denotes the monopole matrix element between two nucleons in the i and j orbits with isospin coupling T . As a result, the tensor force drastically changes the spin-orbit splitting. From the viewpoint of the Nilsson model, the central force and the tensor force are responsible for the evolution of the l^2 and the $l \cdot s$ terms, respectively.

The above-mentioned concept has been quantitatively implemented in the “monopole-based universal interaction” (V_{MU}) which aims at a universal description of shell evolution due to the nuclear force [10]. The original V_{MU} [10] consists of the central force and the tensor force. Its tensor force, the $\pi + \rho$ meson exchange potential, is supported microscopically by the “renormalization persistency” [10, 11] which states that the tensor matrix elements are almost unchanged by the renormalization of the nuclear force. The effective central force includes most of the renormalization effect, and should be quite complicated in principle. However, an analysis of semi-empirical effective interactions for the sd and pf shells shows that the monopole matrix elements for the central force seem to be rather simple. This result motivates us to phenomenologically describe the central force in a simple functional form. In the V_{MU} , a one-range Gaussian central force is employed. This choice is successful in well approximating the central part of the monopole matrix elements of the SDPF-M [12] interaction for the sd shell and GXPF1A [13] interaction for the pf -shell simultaneously. The V_{MU} interaction provides reasonable shell evolutions in various regions of recent interest [10] as far as single-particle-like levels are concerned.

The concept of shell evolution should be verified within reliable many-body calculations because most of the actual states are highly correlated. Our group has been approaching this issue on the basis of large-scale shell-model calculations. In this paper, we report on very recent progress in large-scale shell-model calculations for exotic nuclei from the viewpoint of shell evolution. Methodological and computational aspects of the large-scale shell-model study are covered in this conference by Shimizu [14].

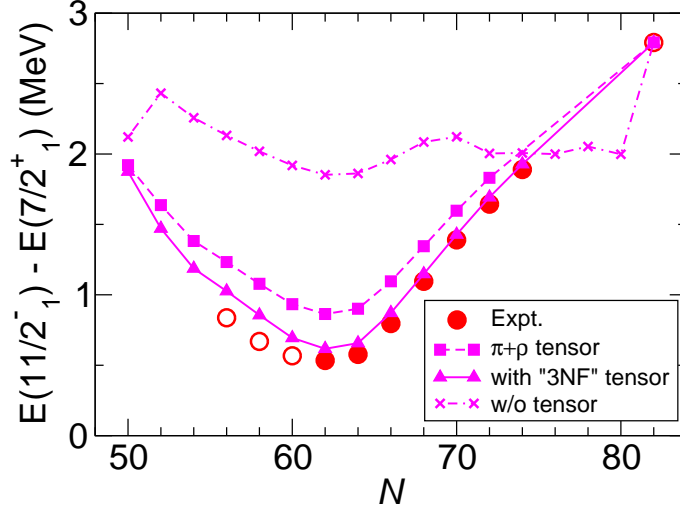


Fig. 2. $11/2^-$ levels in antimony isotopes relative to $7/2^+$ levels. Experimental data are compared to three shell-model calculations using different strengths of the tensor force. The 3NF contribution is phenomenologically introduced by multiplying the $T = 0$ part of the $\pi + \rho$ tensor force by 1.3 according to a recent suggestion [16].

2. Evolution of single-particle-like states

In this section, single-particle-like states in antimony and copper isotopes are examined. Since antimony ($Z = 51$) is located one-major-shell above copper ($Z = 29$), one expects similarity in shell evolution between the two isotope chains. It is shown that correlation cannot be neglected even for those single-particle-like states.

2.1 Antimony isotopes

In antimony isotopes, the $7/2^+$ and the $11/2^-$ levels are observed along a long isotope chain. Those levels are dominated by proton $0g_{7/2}$ and $0h_{11/2}$ single-particle wave functions, respectively, thus providing useful information on shell evolution. Since $0g_{7/2}$ and $0h_{11/2}$ are j_- and j_+ orbits, respectively, the evolution of the energy spacing between those levels is sensitive to the evolution of spin-orbit splitting as pointed out by Schiffer *et al.* [6]. While this single-particle evolution is excellently accounted for by introducing the tensor force [9], significant mixing with core-coupled wave functions could make the situation rather complicated [2].

We perform large-scale shell-model calculations for antimony isotopes from $N = 50$ to $N = 82$ in order to confirm the dominance of the tensor force in the evolution of energy levels within a reliable many-body framework. The valence shell taken in this calculation consists of the $0g_{7/2}$, $1d_{5/2}$, $1d_{3/2}$, $0h_{11/2}$ and $2s_{1/2}$ orbits. The neutron-neutron effective interaction is responsible for constructing good wave functions of tin cores. We use a semi-empirical interaction named SNBG3 [15] for this part, with which low-lying energy levels of tin isotopes are described within a few hundred keV. The proton-neutron effective interaction, on the other hand, controls shell evolution. We take the density-dependent version of the V_{MU} interaction used for the shell-model calculation in the sd - pf shell [17], and apply to it a scaling factor 0.84 for the central part to reproduce good proton separation energies. The proton single-particle energies are determined to fit the energy levels in ^{133}Sb .

In Fig. 2, we compare the $11/2^-$ energy levels relative to $7/2^+$ among three different tensor forces. In each case, the other two-body forces are the same, and the bare proton single-particle energies are readjusted to fit the energy levels in ^{133}Sb . One sees a clear effect of the tensor force. When the tensor

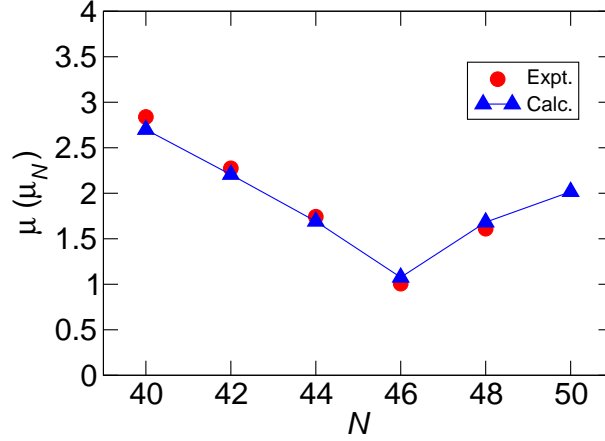


Fig. 3. Magnetic moments in the ground states of Cu isotopes ($3/2^-$ for $40 \leq N \leq 44$, and $5/2^-$ for $46 \leq N \leq 50$) compared between experiment and the MCSM calculation. Experimental data are taken from Refs. [18,20]. In the MCSM calculation, spin g factors are quenched by 0.7, and isovector orbital g factors are added to the free-nucleon g factors by $\delta g_I(\text{IV}) = (\delta g_I(p) - \delta g_I(n))/2 = 0.1$.

force is omitted, the $11/2_1^-$ levels are located almost constantly ~ 2 MeV above the $7/2_1^+$ levels. In this case, dominated by core-coupled states, the $11/2_1^-$ levels contain little proton $0h_{11/2}$ single-particle component. On the other hand, shell-model calculations with the $\pi + \rho$ tensor force lead to reasonable agreement with experiment. When a slightly stronger tensor force is used to include the effect of three-nucleon force as suggested in Ref. [16], agreement with experiment becomes almost perfect.

Although the evolution of the $11/2_1^- - 7/2_1^+$ spacing is strongly influenced by the tensor-force-driven shell evolution, our calculation shows that those energy levels cannot be regarded as single-particle states. The calculated proton spectroscopic factors for those levels are 0.5-0.7 in the mid-shell region ($N \sim 64$), which are much smaller than unity. The increase in correlation towards the mid-shell is strongly supported by the evolution of magnetic moments. The magnetic moments in the $7/2_1^+$ states measured from $N = 70$ to $N = 82$ show a gradual deviation from the Schmidt value with decreasing neutron number from $N = 82$. The present calculation is successful in reproducing this change in parallel with the decrease in spectroscopic factors. It is interesting to see that in spite of significant non-single-particle contribution the evolution of the $11/2_1^- - 7/2_1^+$ spacing is well described with the single-particle evolution due to the tensor force [9]. The calculation shows that this takes place because of cancellation in energy between neutron-neutron correlation and proton-neutron correlation.

2.2 Copper isotopes

A sharp shell evolution between the proton $1p_{3/2}$ and $0f_{5/2}$ orbits is predicted to occur in going from $N = 40$ to $N = 50$, where the neutron $0g_{9/2}$ orbit is filled. This is due to a cooperative effect of the central force and the tensor force: both favor the $\pi 0f_{5/2} - \nu 0g_{9/2}$ monopole matrix elements more than that of $\pi 1p_{3/2} - \nu 0g_{9/2}$ (see Fig. 1). As a result, the proton $0f_{5/2}$ orbit sharply drops down compared to the $1p_{3/2}$ orbit with increasing neutron number as shown in Ref. [10]. This effect is found in the copper isotope chain. The ground states of copper isotopes are known to have $3/2^-$ for $N \leq 44$, whereas the ground state of the $N = 46$ isotope has recently been measured to be $5/2^-$ [18].

As discussed for the antimony isotopes in Sect. 2.1, magnetic moments provide crucial information on to what extent the single-particle state dominates the many-body state. For copper isotopes, the measured magnetic moments have been compared to the single-particle estimates and shell-model calculations in the valence shell consisting of the $1p_{3/2}$, $0f_{5/2}$, $1p_{1/2}$ and $0g_{9/2}$ orbits in Ref. [18]. The

measured moments start to depart from the Schmidt value with increasing neutron number from $N = 40$. Although this tendency is described with the shell-model calculation, a certain deviation from experiment still remains especially in ^{73}Cu . This deviation has disappeared in a later shell-model calculation that activates the proton $0f_{7/2}$ orbit to allow proton excitation across the $Z = 28$ gap [19]. This indicates that very large-scale shell-model calculations are required to describe the structure of copper isotopes because the magic number 28 is more fragile than the ones larger than 28. We carry out such large-scale shell-model calculations in the full pf shell plus the $0g_{9/2}$ and $1d_{5/2}$ orbits using the advanced Monte Carlo shell-model (MCSM) calculation [21]. The effective interaction adopted here is the same as the one used in the study of nickel isotopes (see Sect. 3 and Ref. [22]). As shown in Fig. 3, the magnetic moments calculated with MCSM are in excellent agreement with the experimental data. In this way, we achieve a unified description of nickel and copper isotopes.

While the structure of neutron-rich copper isotopes is well described with large-scale shell-model calculations of Ref. [19] and the present one, it is still ambiguous how much the $0f_{5/2}$ orbit lowers relative to $1p_{3/2}$ in going from $N = 40$ to 50. Rather large changes (4.5-5 MeV) are predicted in Ref. [19] and the JUN45 interaction [23]. On the other hand, V_{MU} and the present calculation lead to smaller changes (3-3.5 MeV). The energy levels in ^{79}Cu , the $N = 50$ isotope, will provide crucial information to quantitatively evaluate the evolution of the $0f_{5/2}$ and $1p_{3/2}$ orbits.

3. Shape coexistence in nickel isotopes and Type II shell evolution

The structure of neutron-rich $N \sim 40$ nuclei has recently been very extensively investigated in RI-beam facilities over the world. One of the interesting issues in this region is a sudden change of nuclear deformation in going down from nickel to smaller proton numbers. This situation is analogous to the so-called island of inversion around ^{32}Mg [4].

Concerning shell evolution, it is argued in Ref. [24] that the $N = 40$ shell gap between the pf shell and $0g_{9/2}$ narrows in going to lower proton numbers in a similar way to the evolution of the $N = 20$ shell gap realized with the SDPF-M interaction [12]. In this usual sense of shell evolution, nickel isotopes have shell gaps large enough to stabilize spherical shapes in their ground states. In contrast, we have proposed an unknown manifestation of shell evolution in Ref. [22]: the shell gap is not necessarily fixed in a designated nucleus but can evolve depending on configuration. Here we consider how the shell evolution within a nucleus influences shape coexistence in nickel isotopes. The spherical configurations in nickel isotopes are the filling configurations, and produce relatively large $Z = 28$ and $N = 40$ shell gaps. On the other hand, the deformed configurations are associated with particle-hole excitation across the $N = 40$ shell gap (e.g., $4p\text{-}4h$ configuration for the prolate state). Thus, the deformed configurations have more neutron particles in the $0g_{9/2}$ orbit and neutron holes in the $0f_{5/2}$ and $1p_{1/2}$ orbits than the spherical configurations. The occupation in the $j_>$ orbit and absence in the $j_<$ orbit work coherently to reduce the spin-orbit splitting of proton orbits due to the tensor force. Consequently, protons are more easily excited into the upper pf shell, and deformation is promoted. This is rather different from the conventional one-body potential picture such as the Nilsson model in which the shell structure is constant within a fixed proton-neutron number. The shell evolution which occurs within a nucleus depending on configuration is called Type II shell evolution to distinguish from the usual (Type I) shell evolution which is based on the filling configurations.

In Ref. [22], a unified description of nickel isotopes from $N = 28$ to $N = 50$ has been given with the MCSM calculations in the full pf shell plus the $0g_{9/2}$ and $1d_{5/2}$ orbits. We have developed a new method to visualize shape fluctuation in each strongly correlated many-body wave function by utilizing the intrinsic shapes of MCSM basis states [22]. With this method, we have clearly shown that spherical-oblate-prolate shape coexistence occurs in ^{68}Ni . Type II shell evolution is crucial in stabilizing deformation. Similar shape coexistence is predicted for surrounding nuclei, which is of great interest to confirm in forthcoming experiments.

4. Evolution of the new $N = 34$ magic number

It has been predicted in 2001 that a new $N = 34$ magic number appears around calcium isotopes as a large shell gap between $1p_{1/2}$ and $0f_{5/2}$ [25]. The mechanism of its appearance is the same as that of the $N = 16$ magic number for the sd shell [12, 26]: strong attraction between a proton in a $j_>$ orbit ($0d_{5/2}$ or $0f_{7/2}$) and a neutron in a $j_<$ orbit ($0d_{3/2}$ or $0f_{5/2}$) produces a large shell gap below the neutron $j_<$ orbit when no protons occupy the $j_>$ orbit (i.e., oxygen or calcium). As for the pf shell, the $\nu 0f_{5/2}$ orbit is known to be located between $\nu 1p_{3/2}$ and $\nu 1p_{1/2}$ in nickel isotopes. When protons are removed from $0f_{7/2}$, the $\nu 0f_{5/2}$ orbit is shifted up above the $\nu 1p_{1/2}$ orbit. The $N = 32$ shell gap, the one between $\nu 1p_{3/2}$ and $\nu 1p_{1/2}$, thus appears first. Several evidences for the $N = 32$ magic number have been found in chromium, titanium, and calcium isotopes [27–29]. On the other hand, the $N = 34$ shell gap is not large enough to make a closed-shell structure in chromium and titanium isotopes [27, 30]. The occurrence of the $N = 34$ magic number has been observed quite recently [31] from the 2_1^+ level in ^{54}Ca [31] which is much higher than the ones in non-magic nuclei such as $^{42-46,50}\text{Ca}$. Those experimental results indicate that the $N = 34$ magic number is quite localized because of a sharp evolution of the $\nu 0f_{5/2}$ orbit as a function of the proton number.

Although the strength of the $N = 34$ shell gap cannot be directly measured, it is estimated from the comparison of energy levels between experiment and shell-model calculations. We take the GXPFI1B [32] and GXPFI1Br [31] interactions for the full pf -shell calculations. The GXPFI1B interaction gives a good description of neutron-rich calcium isotopes systematically, but its 2_1^+ level in ^{54}Ca is 0.6 MeV too high. To remedy this small discrepancy in a simple way, the GXPFI1Br interaction is proposed [31] by minimally modifying the GXPFI1B interaction, $\delta \nu_{1p_{3/2}, 0f_{5/2}}^{T=1} = -0.15$ MeV, in order to reproduce the 2_1^+ level in ^{54}Ca . The resulting $N = 34$ shell gap for the GXPFI1Br interaction is 2.66 MeV. The GXPFI1Br interaction improves not only the 2_1^+ level in ^{54}Ca but also some other energy levels in calcium and scandium isotopes which are dominated by the configurations involving $0f_{5/2}$. Thus, the $N = 34$ shell gap in calcium isotopes is estimated to be ~ 2.6 MeV, which is close to the $N = 32$ shell gap.

Once a large $N = 34$ shell gap in calcium isotopes is established, it is a natural question to ask how this magic structure evolves and how the evolution affects observables in the more exotic region, i.e., isotopes with less proton numbers. Since the proton valence shell moves to the sd shell, the proton-neutron monopole matrix elements relevant to the evolution of the $N = 34$ shell gap are $\pi 0d_{3/2}-\nu 1p_{1/2}$ vs. $\pi 0d_{3/2}-\nu 0f_{5/2}$ and $\pi 1s_{1/2}-\nu 1p_{1/2}$ vs. $\pi 1s_{1/2}-\nu 0f_{5/2}$. Concerning the matrix elements associated with $\pi 0d_{3/2}$, the $\nu 0f_{5/2}$ orbit is more attractive than the $\nu 1p_{1/2}$ orbit for the central force, but is more repulsive for the tensor force. The matrix elements regarding $\pi 1s_{1/2}$ orbit favor $\nu 1p_{1/2}$ more than $\nu 0f_{5/2}$ in the central channel, and vanish in the tensor channel. Thus, the evolution of the $N = 34$ magic number towards smaller proton numbers is difficult to predict only from this qualitative discussion.

Those monopole matrix elements are quantitatively estimated on the basis of the SDPF-MU interaction [17], whose cross-shell part consists of the V_{MU} interaction. Although its cross-shell monopole matrix elements are quite reasonable on the whole in view of its descriptive power [17], there is room for improvement on the central matrix element between $1s$ and $1p$ because of some discrepancy in the evolution of the $\pi 1s_{1/2}$ hole levels in potassium isotopes beyond $N = 28$ [33]. The binding energies and energy levels in neutron-rich potassium isotopes strongly constrain the amplitude of the central monopole matrix elements between proton $0d/1s$ and neutron $0f/1p$ orbits. Here we shift the $\pi 1s-\nu 1p$ central monopole matrix elements by +0.3 MeV so as to achieve good agreement with experimental energies in potassium isotopes. In addition to this change, the SDPF-MU interaction is modified by replacing its pf -shell part with the GXPFI1Br interaction.

The resulting modified SDPF-MU interaction predicts the enhancement of the $N = 34$ shell gap towards lower proton numbers: it ends up with 3.9 MeV at ^{48}Si . Although the evolution of the $N = 34$

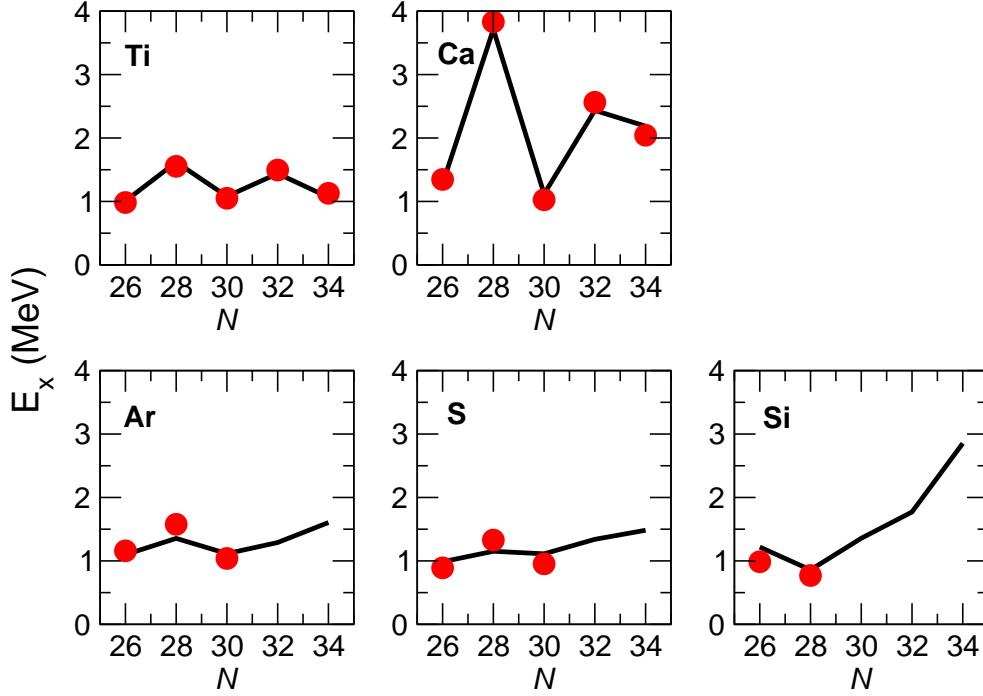


Fig. 4. 2_1^+ energy levels in neutron-rich titanium, calcium, argon, sulfur, and silicon isotopes compared between experiment (circles) and theory (lines).

shell gap has not been observed for $N = 34$ isotones, the shell gap between $\nu 1p_{1/2}$ and $\nu 0f_{5/2}$ appears to somewhat enhance in going from calcium to silicon in terms of the distribution of spectroscopic factors in $N = 20$ isotones [34]. According to shell evolution due to the monopole interaction, if the $N = 34$ shell gap enlarges for the $N = 20$ core to some extent, it enlarges for the $N = 34$ core to the same degree. Hence, it is likely that the $N = 34$ shell gap enlarges towards silicon isotopes. The effect of the enhanced $N = 34$ shell gap can be detected experimentally. In Fig. 4, the 2_1^+ energy levels in neutron-rich titanium, calcium, argon, sulfur and silicon isotopes are compared between the experimental data and the shell-model calculations using the modified SDPF-MU interaction. While the 2_1^+ energy in titanium isotopes decreases in going from $N = 32$ to $N = 34$, the ones in argon, sulfur and silicon isotopes increase due to their large $N = 34$ shell gaps. In particular, ^{48}Si is predicted to be a new doubly magic nucleus, having a 2_1^+ level located at ~ 3 MeV. It is of great interest to verify this prediction in current and future RI-beam facilities.

5. Conclusion

We have performed large-scale shell-model calculations for exotic nuclei ranging from light to medium-heavy regions to investigate shell evolution. Currently, the central and the tensor forces are regarded as two major sources that cause shell evolution in the proton-neutron channel. Since those two forces cause rather different evolutions in character, it is possible to extract the tensor-force-driven shell evolution from experimental data concerning exotic nuclei. Large-scale shell-model calculations are of great help for this purpose. We have calculated single-particle-like levels in antimony and copper isotopes systematically. Although those levels suffer much correlation, their evolutions are strongly dominated by shell evolution. As a result, the current understanding of shell evolution implemented in V_{MU} is confirmed. We point out that shape coexistence in nickel isotopes is stabilized

through a new manifestation of shell evolution, Type II shell evolution. We finally predict that the new $N = 34$ magic number recently found in ^{54}Ca persists with decreasing proton numbers. The $N = 34$ shell gap is predicted to enlarge there, and measuring the 2_1^+ energies in very neutron-rich argon, sulfur, and silicon isotopes will provide crucial information to probe the predicted evolution.

Acknowledgments

This work was supported in part by JSPS KAKENHI Grant Numbers 21740204 and 23244049 and by the HPCI System Research Project (hp120284, hp130024 and hp140210). This work is a part of the CNS-RIKEN joint research project on large-scale nuclear-structure calculations.

References

- [1] A. Gade and T. Glasmacher: Prog. Part. Nucl. Phys. **60** (2008) 161.
- [2] O. Sorlin, M.-G. Porquet: Prog. Part. Nucl. Phys. **61** (2008) 602.
- [3] T. Otsuka: Phys. Scr. T **152** (2013) 014007.
- [4] E.K. Warburton, J.A. Becker, and B.A. Brown: Phys. Rev. C **41** (1990) 1147.
- [5] R. V. F. Janssens: Nature **459** (2009) 1069, and references therein.
- [6] J. P. Schiffer *et al.*: Phys. Rev. Lett. **92** (2004) 162501.
- [7] R. K. Bansal and J. B. French: Phys. Lett. **11** (1964) 145; A. Poves and A. Zuker: Phys. Rep. **70** (1981) 235.
- [8] K. Heyde and J. L. Wood: J. Phys. G **17** (1991) 135.
- [9] T. Otsuka, T. Suzuki, R. Fujimoto, H. Grawe, and Y. Akaishi: Phys. Rev. Lett. **95** (2005) 232502.
- [10] T. Otsuka *et al.*: Phys. Rev. Lett. **104** (2010) 012501.
- [11] N. Tsunoda, T. Otsuka, K. Tsukiyama, and M. Hjorth-Jensen, Phys. Rev. C **84** (2011) 044322.
- [12] Y. Utsuno, T. Otsuka, T. Mizusaki, and M. Honma: Phys. Rev. C **60** (1999) 054315.
- [13] M. Honma, T. Otsuka, B. A. Brown, and T. Mizusaki: Eur. Phys. J. A **25**, s01 (2005) 499.
- [14] N. Shimizu *et al.*: contribution to this conference.
- [15] SNBG3 is a variant of the SNBG1 interaction [M. Honma *et al.*, RIKEN Accelerator Progress Report **45** (2011) 35], taking also the 3_1^- levels into consideration in the fitting procedure.
- [16] M. Kohn: Phys. Rev. C **88** (2013) 064005.
- [17] Y. Utsuno *et al.*: Phys. Rev. C **86** (2012) 051301(R).
- [18] K. T. Flanagan *et al.*: Phys. Rev. Lett. **103** (2009) 142501.
- [19] K. Sieja and F. Nowacki: Phys. Rev. C **81** (2010) 061303(R).
- [20] U. Köster *et al.*: Phys. Rev. C **84** (2011) 034320.
- [21] N. Shimizu *et al.*: Prog. Theor. Exp. Phys. **2012** (2012) 01A205.
- [22] Y. Tsunoda, T. Otsuka, N. Shimizu, M. Honma, and Y. Utsuno: Phys. Rev. C **89** (2014) 031301(R).
- [23] M. Honma, T. Otsuka, T. Mizusaki, and M. Hjorth-Jensen: Phys. Rev. C **80** (2009) 064323.
- [24] S. M. Lenzi, F. Nowacki, A. Poves, and K. Sieja: Phys. Rev. C **82** (2010) 054301.
- [25] T. Otsuka *et al.*: Phys. Rev. Lett. **87** (2001) 082502.
- [26] A. Ozawa, T. Kobayashi, T. Suzuki, K. Yoshida, and I. Tanihata: Phys. Rev. Lett. **84** (2000) 5493.
- [27] J.I. Prisciandaro *et al.*: Phys. Lett. B **510** (2001) 17.
- [28] R.V.F. Janssens *et al.*: Phys. Lett. B **546** (2002) 55.
- [29] A. Huck *et al.*: Phys. Rev. C **31** (1985) 2226.
- [30] S. N. Liddick *et al.*: Phys. Rev. Lett. **92** (2004) 072502.
- [31] D. Steppenbeck *et al.*: Nature **502** (2013) 207.
- [32] M. Honma, T. Otsuka, and T. Mizusaki: RIKEN Accelerator Progress Report **41** (2008) 32.
- [33] J. Papuga *et al.*: Phys. Rev. Lett. **110** (2013) 172503.
- [34] G. Burgunder *et al.*: Phys. Rev. Lett. **112** (2014) 042502.